Supporting Information

Stouf et al. 10.1073/pnas.1304080110

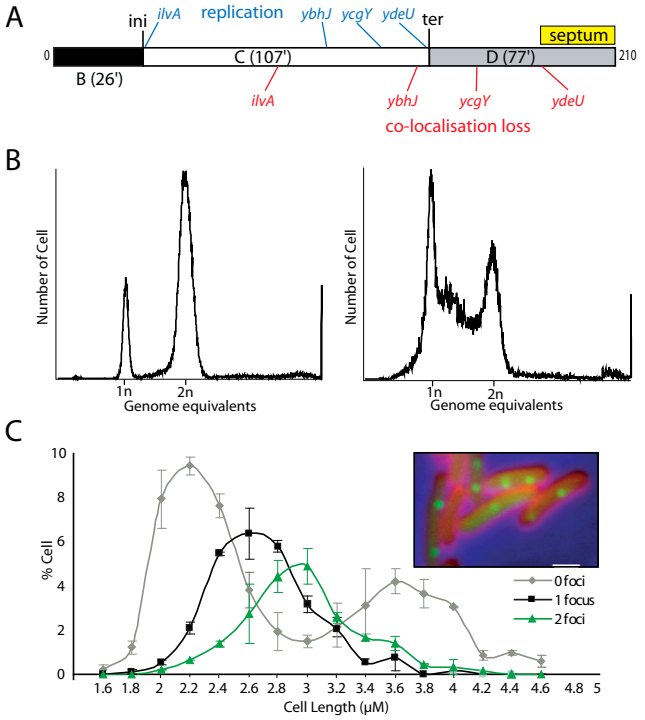

Fig. S1. Cell cycle of strain LN2666. (*A*–*C*) Cell-cycle periods were calculated from the doubling time of strain LN2666 (Table S1) grown in M9-alanine medium (DT, 210 min) (*A*), the flow cytometry patterns shown in *B*, and the number of SSB-Ypet foci in individual cells shown in *C*. ini, mean time of replication initiation; ter, mean time of replication termination. (*A*) The mean number of replication origins per cell (n_{ori}) was counted after rifampicin/cephalexin treatment of exponentially growing cells (B at left of bar). The C+D period was calculated as ($DT \times \ln(n_{ori})/\ln 2$). The duration of the C period was estimated from the pattern of SSB-Ypet foci in both snapshot (*C*) and time-lapse analysis. Cell-cycle periods were in good agreement with those previously published for strain MG1655 in these growth conditions (1). The mean times of loci replication (indicated in blue) were calculated from their distance to *oriC* and the replication fork velocity inferred from the duration of the C period (0.36 kb/s). The mean times of sister loci colocalization loss were calculated from the mean number of foci per cell (n_f) as $t = DT \times \ln(n_f)/\ln 2$, where t is the time separating cell division from colocalization loss. The time of septum constriction (yellow bar) was calculated from the ratio of cells harboring a constricting septum using the same formula. (*B*) For flow cytometry analysis, cells were grown in M9-alanine medium at 30 °C to $OD_{600} = 0.2$. Rifampicin (300 μg/mL) and cephalexin (10 μg/mL) were added when needed, followed by 4-h incubation. Cells then were fixed using cold ethanol [74% (vol/vol) final concentration] and stored at 4 °C. Fixed cells were washed twice with 100 μL of cold staining buffer (10 mM Tris, pH7.4, 10 mM $MgCl_2$), and 400 μL of a 0.4% Syto16 solution (Invitrogen) was added for 1 min before analysis using a BD FACSCalibur flow cytometer. Genome equivalents were determined using cells in stationary phase. Acquisitions were done using CellQuest Pro software. (*C*) Cells containing a SSB-Ypet fusion were classified depending on their number of foci and binned in 2-mM cell length classes. The percentage of cells in each class (y-axis) was plotted against cell length (x-axis).

1. Michelsen O, Teixeira de Mattos MJ, Jensen PR, Hansen FG (2003) Precise determinations of C and D periods by flow cytometry in Escherichia coli K-12 and B/r. *Microbiology* 149(Pt 4): 1001–1010.

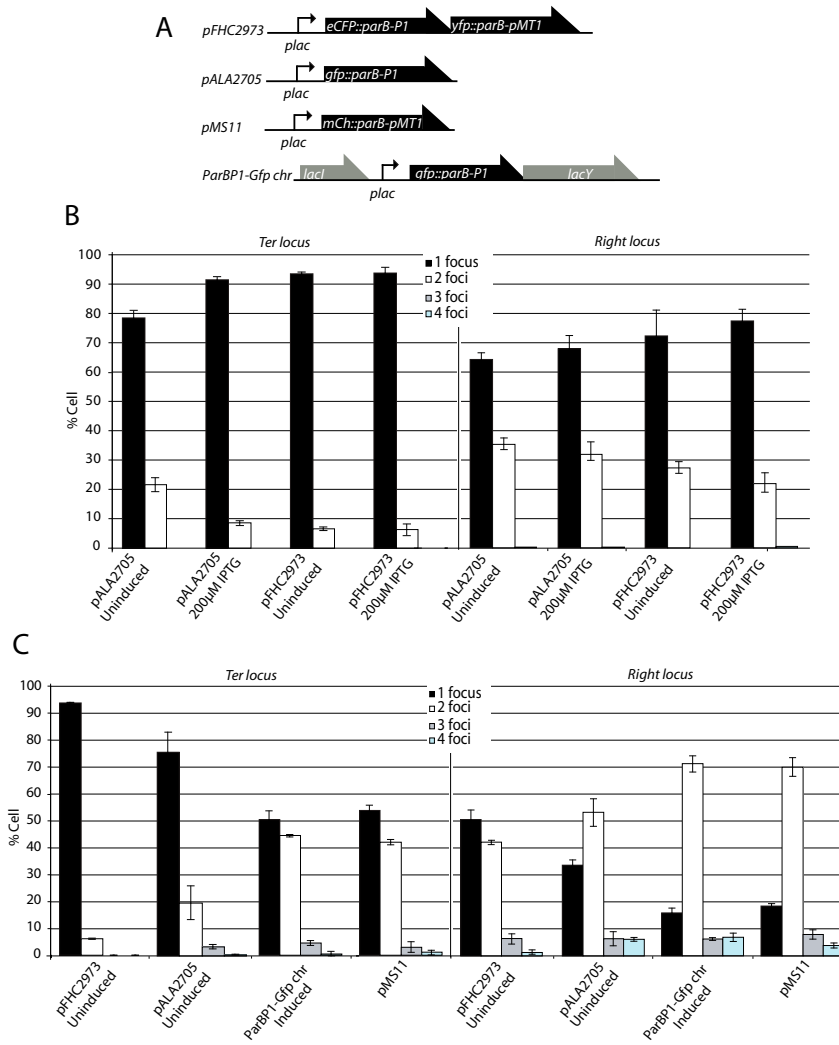

Fig. S2. Comparison of loci visualization systems. (*A*) Plasmids and chromosomal constructs producing ParB-fusion proteins. (*B* and *C*) Percentage of cells harboring the indicated number of foci of the *ydgJ* (*ter*) and *ydhC* (right) loci tagged with $parS_{pMT1}$ (pMS11) or $parS_{P1}$ (other lanes), when visualized using the different localization systems shown in *A*. (*B*) Cells were grown in M9 medium containing alanine as a carbon source (0.2%), thiamine (1 µg/mL), thymine (2 µg/mL), and leucine (2 µg/mL). (*C*) Cells were grown in the same medium, except that glycerol (0.2%) and casamino acids (0.2% final concentration) replaced alanine as a carbon source.

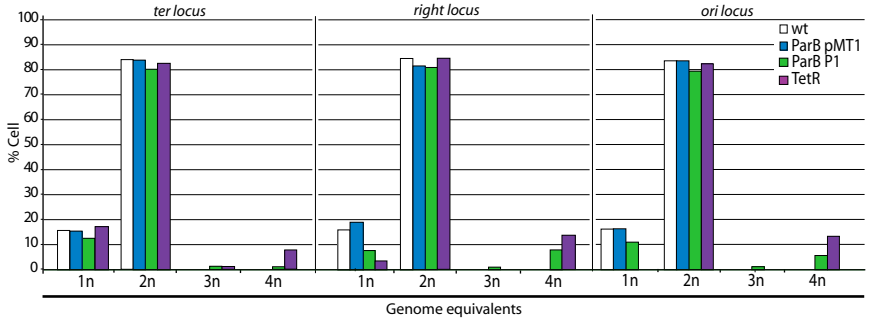

Fig. S3. Effects of loci visualization systems on the cell cycle. Wild-type LN2666 (open bars) and strains with a ter (*ydgJ*), right (*ybhJ*), or ori (*ilvA*) locus tagged with the indicated systems were grown in M9-alanine medium to exponential phase. Inductors were added as indicated in *Materials and Methods*; then cells were treated with cephalexin and rifampicin for 3 h before flow cytometry analysis (see Fig. S1). The percentages of cells harboring the indicated genome equivalents are plotted.

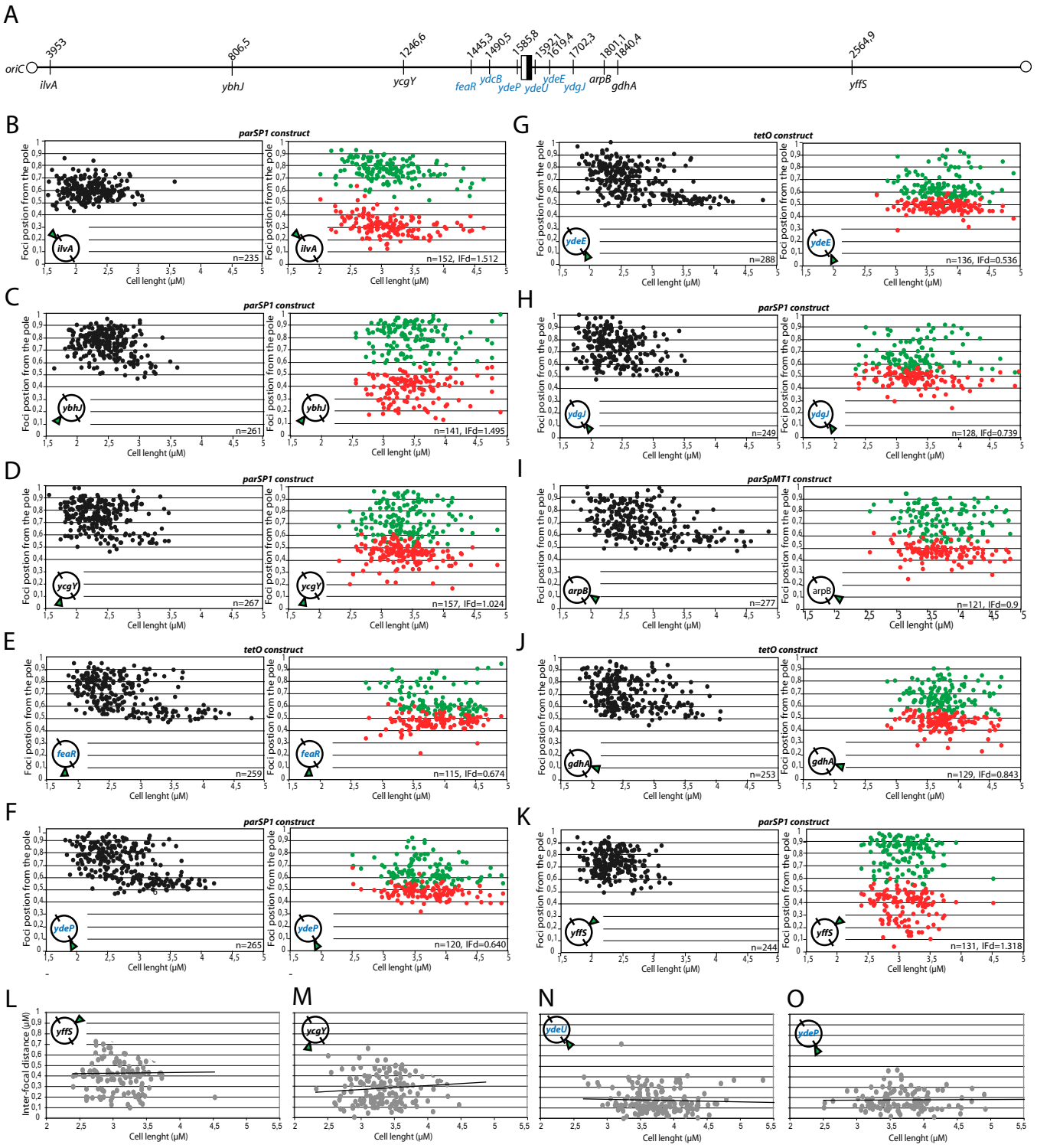

Fig. S4. Positioning of chromosome loci. (*A*) Map of the loci used, with coordinates indicated (see also Table S3). The black and white box represents the *dif* site, and the open circle represents the replication origin. Loci inside the region of high FtsK activity are shown in blue (1). (*B–K*) Position of the indicated foci of loci tagged with the indicated system from their farthest pole (*y*-axis) as a function of cell length (*x*-axis). (*Left*) Cells with a single focus (black dots). (*Right*) Cells with two foci (red and green dots). Loci positions are drawn on a circular chromosome map. The number of cells analyzed (*n*) and the mean interfocal distance for cells with two foci (IFd) are indicated. (*L–O*) The interfocal distance in cells with two foci (*y*-axis) was plotted as a function of cell length for the indicated loci (*x*-axis).

1. Deghorain M, et al. (2011) A defined terminal region of the E. coli chromosome shows late segregation and high FtsK activity. *PLoS ONE* 6(7):e22164.

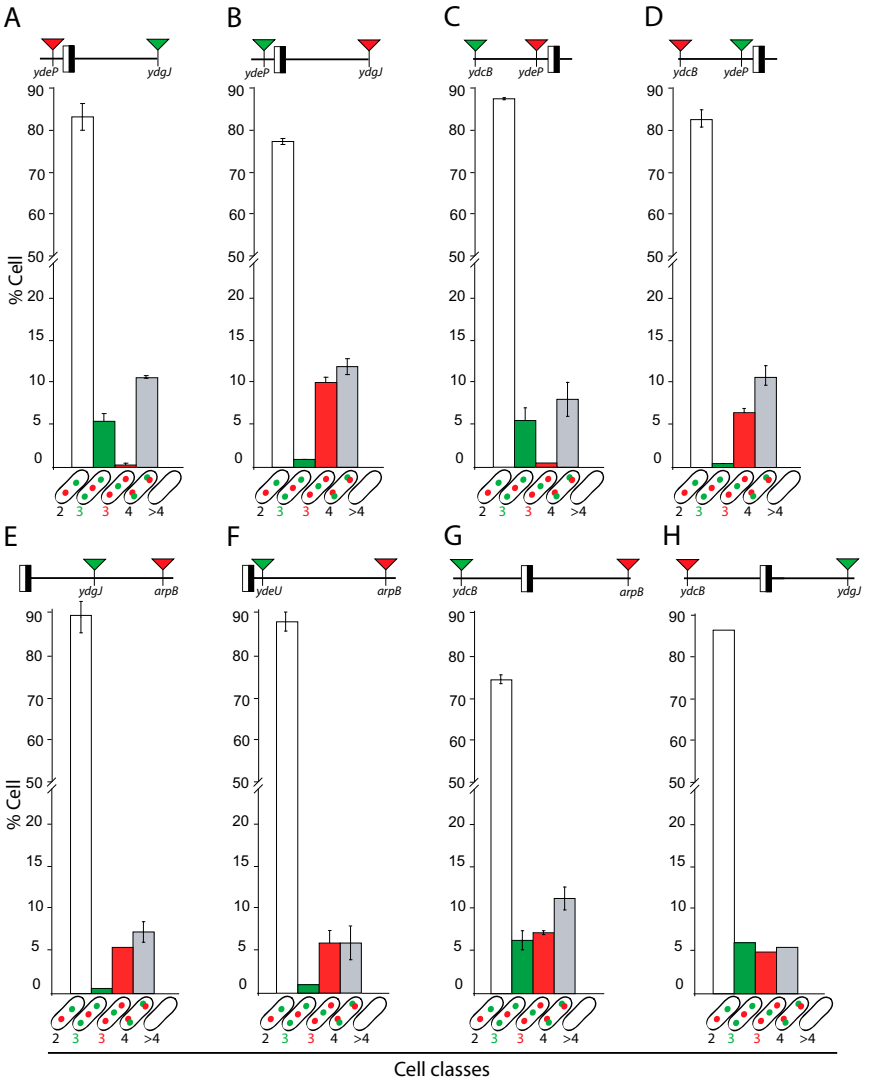

Fig. S5. Order of segregation of *ter* loci in wild-type strains. (*A*–*H*) Tagged loci are indicated with their position relative to *dif* (the black and white box). Red arrowheads indicate a $parS_{pMT1}$ tag, and green arrowheads indicate a $parS_{P1}$ tag. Cells were classified by the number of foci of each locus (shown in cartoons on the *x*-axis; the empty cell indicates cells that fall in none of the first four categories). Bars show the mean percentage of each category in the population (*y*-axis) with individual measured ranges. Data reflect at least two independent experiments and more than 600 cells.

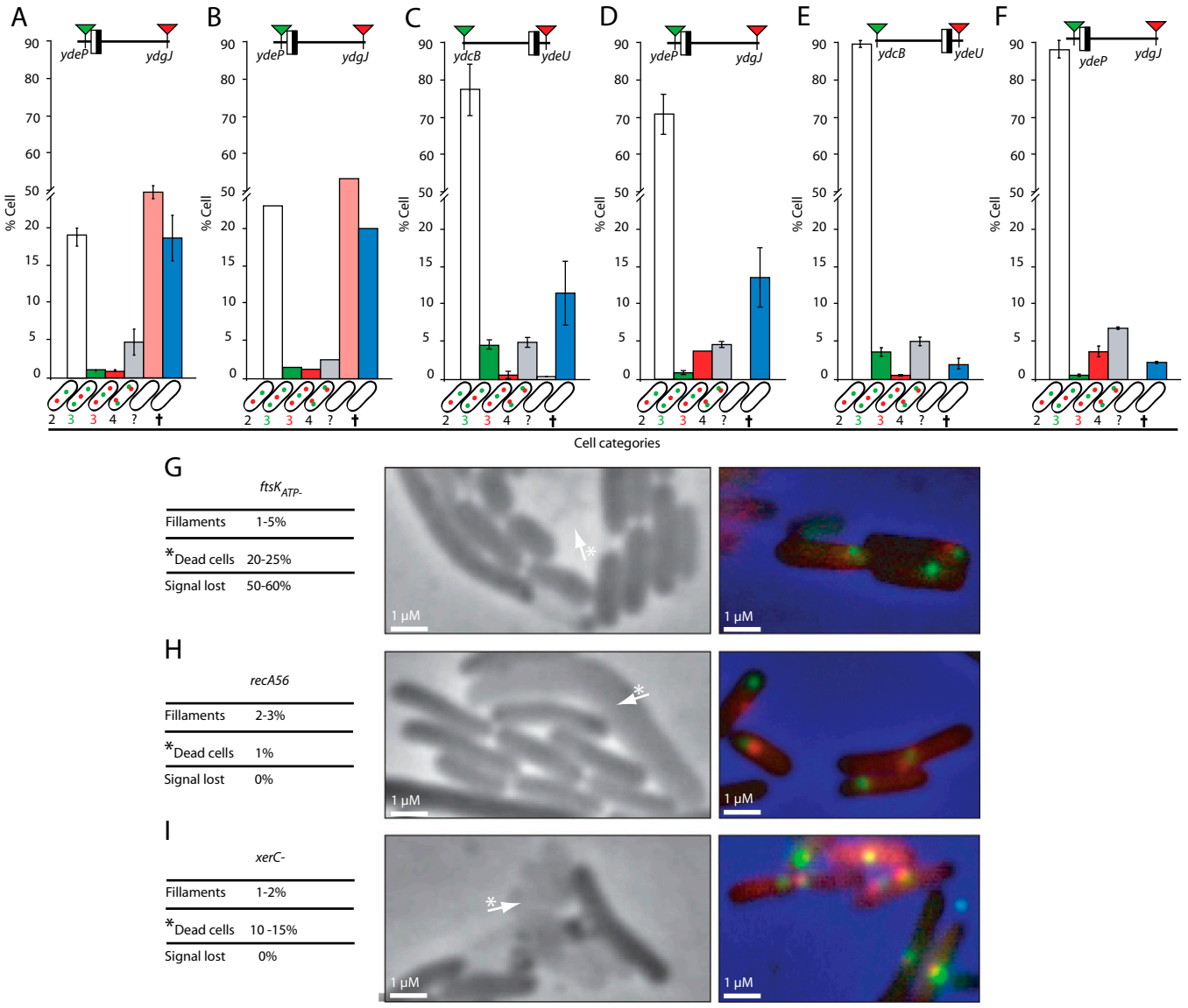

Fig. S6. Order of segregation of *ter* loci in strains carrying mutations. (*A*–*F*) Tagged loci are indicated with their position relative to *dif* (the black and white box). Red arrowheads indicate a $parS_{pMT1}$ tag, and green arrowheads indicate a $parS_{P1}$ tag. Cells were classified by the number of foci of each locus (shown in cartoons on the *x*-axis; the empty cell indicates cells that fall in none of the first four categories; blue bars indicate dead cells). Bars show the mean percentage of each category in the population (*y*-axis) with individual measured ranges. Data reflect at least two independent experiments and more than 600 cells. (*A*) $ftsK_{ATP-}$ strain. (*B*) Δ($ftsK_C$) strain. (*C* and *D*) $xerC^-$ strains. (*E* and *F*) $xerC^-$ $recA^-$ strains. (*G* and *H*) Analysis of micrographs of strains carrying the indicated mutation with chosen examples. Fluorescent signals were absent in about half cells in $ftsK_{ATP-}$ and Δ($ftsK_C$) strains (most cells correspond to the salmon bar in *A* and *B*). Examples of dead (empty) cells are indicated by the white arrows.

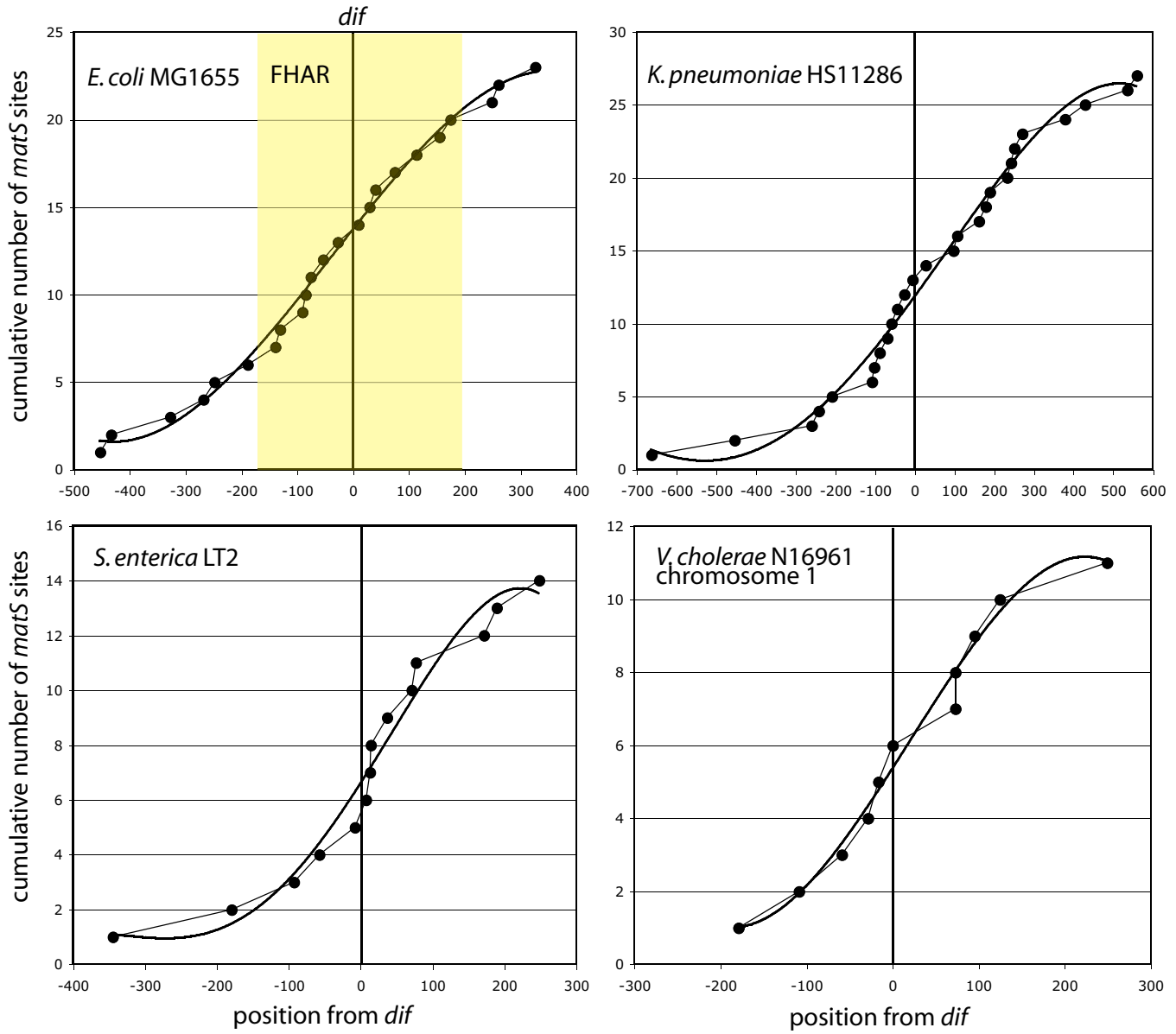

Fig. S7. Repartition of *matS* sites in *ter* regions. Panels show cumulative plots of *matS* sites (GTGACYNRGTCAC) in the chromosomal *ter* regions of the indicated bacteria (*y*-axis) as a function of their distance from the *dif* site (*x*-axis). Cumulative plots fit the sigmoid curves shown better than linear curves, indicating that *matS* sites tend to cluster in restricted regions around *dif*. In the case of *Escherichia coli* MG1655, the region of higher slope corresponds to the FtsK high-activity region (FHAR, shown in yellow).

Table S1. Strains used

Strain	Relevant genotype	Comments
Reference strains		
LN2666	W1485 W1485 F- leu thyA thi deoB or C supE rpsL (StR)	Wild-type strain (1)
MS112	LN2666 del(lacZ)::gfp-parBP1	Integration of gfp-parB P1 using pMS8*
MS154	LN2666 del(araB)::tetR-gfp	Transfer of tetR-gfp (Gift from Jean-Yves Bouet, Centre National de la Recherche Scientifique, Toulouse, France)[†]
JCT9	LN2666 SSB-Ypet	Transfer of ssb-Ypet (2)
Single-locus tagged strains		
MS158	MS112 inter(ilvA;ilvY)::parS P1-Kn	Integration of parS P1 at the ilvA-ilvY locus using pMS59*
MS159	MS112 inter(yffS;eutA)::parS P1-Kn	Integration of parS P1 at the yffS-eutA locus using pMS56*
MS182	MS112 inter(ybhJ;ybhC)::parS P1-Kn	Integration of parS P1 at the ybhJ-ybhC locus using pMS58*
MS165	MS154 inter(ybhJ;ybhC)::tetO-Gm	Integration of tetO arrays at the ybhJ-ybhC locus using pMS53*
MS144	MS112 inter(ycgY;treA)::parS P1-Kn	Integration of parS P1 at the ycgY-treA locus using pMS55*
MS167	MS154 inter(ycgY;treA)::tetO-Gm	Integration of tetO arrays at the ycgY-treA locus using pMS49*
MS168	MS154 inter(ydbL;feaR)::tetO-Gm	Integration of tetO arrays at the ydbL-feaR locus using pMS47*
MS447	MS112 inter(ydcB;trg)::parS P1	Integration of parS P1 at the ydcB-trg locus using λRed Recombination[‡,§]
MS11	LN2666 inter(ydcB;trg)::parS pMT1	Integration of parS pMT1 at the ydcB-trg locus using λRed Recombination[‡,§]
MS471	MS112 inter(ydeP;ydeQ)::parS P1	Integration of parS P1 at the ydeP-ydeQ locus using λRed Recombination[‡,§]
MS3	LN2666 inter(ydeP;ydeQ)::parS pMT1	Integration of parS pMT1 at the ydeP-ydeQ locus using λRed Recombination[‡,§]
MS472	MS112 inter(ydeU;ydeK)::parS P1	Integration of parS P1 at the hipB-ydeU locus using λRed Recombination[‡,§]
MS5	LN2666 inter(ydeU;ydeK)::parS pMT1	Integration of parS pMT1 at the ydeU-ydeK locus using λRed Recombination[‡,§]
MS163	MS154 inter(ydeE;ydeH)::tetO-Gm	Integration of tetO arrays at the ydeE-ydeH locus using pMS46*
MS146	MS112 inter(ydgJ;ydgT)::parS P1-Kn	Integration of parS P1 at the ydgJ-ydgT locus using λRed Recombination[‡,]
MS164	MS154 inter(ydgJ;ydgT)::tetO-Gm	Integration of tetO arrays at the ydgJ-ydgT locus using pMS48*
MS15	LN2666 inter(ydgJ;ydgT)::parS pMT1	Integration of parS pMT1 at the ydgJ-ydgT locus using λRed Recombination[‡,§]
MS166	MS154 inter(gdhA;ynjL)::tetO-Gm	Integration of tetO arrays at the gdhA-ynjL locus using pMS50*
MS294	MS112 inter(ydgJ;ydgT)::parS pMT1 + pMS11	Integration of parS pMT1 at the ydgJ-ydgT locus using λRed Recombination([‡,§]
MS406	MS112 inter(ybhJ;ybhC::parS pMT1 + pMS11	Integration of parS pMT1 at the ybhC-ybhJ locus using λRed Recombination[‡,§]
MS322	LN2666 inter(ybhJ;ybhC)::parS P1 + pFHC2973	Transfer of parS P1 from MS182 in LN2666[†,§], Transformation with pFHC2973
MS323	LN2666 inter(ybhJ;ybhC)::parS P1 + pALA2705	Transfer of parS P1 from MS182 in LN2666[†,§], Transformation with pALA2705
MS324	LN2666 inter(ydgJ;ydgT)::parS P1 + pFHC2973	Transfer of parS P1 from MS146 in LN2666[†,§], Transformation with pFHC2973
MS325	LN2666 inter(ydgJ;ydgT)::parS P1 + pALA2705	Transfer of parS P1 from MS146 in LN2666[†,§], Transformation with pALA2705
MS560	LN2666 inter(ydgJ;ydgT)::parS P1-Kn + ssb-mCherry FRT-Cm-FRT	Transfer of ssb-mCherry (Gift from Jean-Yves Bouet, Toulouse) to MS146[†]
MS561	LN2666 inter(ycgY;treA)::parS P1-Kn + ssb-mCherry FRT-Cm-FRT	Transfert of ssb-mCherry (Gift from Jean-Yves Bouet, Toulouse) in MS144[†]
Double-loci tagged strains		
MS291	MS112 inter(ilvA;ilvY)::parS P1-Kn, inter(ydeU;ydeK)::parS pMT1 + pMS11	Transfer of parS pMT1 from MS5 in MS158[†,§], Transformation with pMS11
MS297	MS112 inter(yffS;eutA)::parS P1-Kn, inter(ydeU;ydeK)::parS pMT1 + pMS11	Transfer of parS pMT1 from MS5 in MS159[†,§], Transformation with pMS11
MS292	MS112 inter(ybhJ;ybhC)::parS P1-Kn, inter(ydeU;ydeK)::parS pMT1 + pMS11	Transfer of parS pMT1 from MS5 in MS182[†,§], Transformation with pMS11

Table S1. Cont.

Strain	Relevant genotype	Comments
MS279	MS112 inter(ycgY;treA)::parS P1-Kn, inter(ydeU;ydeK)::parS pMT1 + pMS11	Transfer of parS pMT1 from MS5 in MS144[†,§], Transformation with pMS11
MS281	MS112 inter(ydgJ;ydgT)::parS P1-Kn, inter(ydeU;ydeK)::parS pMT1 + pMS11	Transfer of parS pMT1 from MS5 in MS146[†,§], Transformation with pMS11
MS425	MS112 inter(trg;ydcI)::parS P1, inter(ydeU;ydeK)::parS pMT1 + pMS11	Transfer of parS pMT1 from MS5 in MS447[†,§], Transformation with pMS11
MS71	MS112 inter(trg;ydcI)::parS pMT1, inter(ydeU;ydeK)::parS P1 + pMS11	Transfer of parS pMT1 from MS11 in MS472[†,§], Transformation with pMS11
MS402	MS112 inter(ydeP;ydeQ)::parS P1, inter(ydgJ;ydgT)::parS pMT1 + pMS11	Transfer of parS pMT1 from MS15 in MS471[†,§], Transformation with pMS11
MS83	MS112 inter(ydeP;ydeQ)::parS pMT1, inter(ydgJ;ydgT)::parS P1 + pMS11	Transfer of parS pMT1 from MS3 in MS144[†,§], Transformation with pMS11
MS107	MS112 inter(ydeU;ydeK)::parS P1, inter(ydgJ;ydgT)::parS pMT1 + pMS11	Transfer of parS pMT1 from MS15 in MS472[†,§], Transformation with pMS11
MS89	MS112 inter(ydeP;ydeQ)::parS P1, inter(trg, ydcI)::parS pMT1 + pMS11	Transfer of parS pMT1 from MS11 in MS471[†,§], Transformation with pMS11
MS95	MS112 inter(ydeP;ydeQ)::parS pMT1, inter(trg, ydcI)::parS pMT1 + pMS11	Transfer of parS pMT1 from MS11 in MS447[†,§], Transformation with pMS11
Strains carrying ftsK, recA, xerC, or matP mutations		
MS450	MS112 inter(trg;ydcI)::parS P1, inter(ydeU;ydeK)::parS pMT1, matP::FRT-Kn-FRT + pMS11	Transfer of matP FRT-Kn-FRT from JW0939 of the KEIO collection[†,§,¶]
MS451	MS112 inter(ydeP;ydeQ)::parS P1, inter(ydgJ;ydgT)::parS pMT1, matP::FRT-Kn-FRT + pMS11	Transfer of matP FRT-Kn-FRT[†,§]
MS367	MS112 inter(ycgY;treA)::parS P1, inter(ydeU;ydeK)::parS pMT1, matP::FRT-Kn-FRT + pMS11	Transfer of matP FRT-Kn-FRT[†,§]
MS480	MS112 inter(trg;ydcI)::parS P1, inter(ydeU;ydeK)::parS pMT1, ftsK-KOPSblind-Cm + pMS89	Transfer of ftsK-KOPSblind-Cm from VSO4 (3)[†,§]
MS481	MS112 inter(ydeP;ydeQ)::parS P1, inter(ydgJ;ydgT)::parS pMT1, ftsK-KOPSblind-Cm + pMS89	Transfer of ftsK-KOPSblind-Cm from VSO4(3)[†,§]
MS253	MS112 inter(ycgY;treA)::parS P1, inter(ydeU;ydeK)::parS pMT1, ftsK-KOPSblind-Cm + pMS89	Transfer of ftsK-KOPSblind-Cm from VSO4(3)[†,§]
MS478	MS112 inter(ydeU;ydeK)::parS pMT1, inter(ydgJ;ydgT)::parS P1, ftsK-KOPSblind-Cm + pMS89	Transfer of ftsK-KOPSblind-Cm from VSO4(3)[†,§]
MS479	MS112 inter(ydeU;ydeK)::parS P1, inter(ydgJ;ydgT)::parS pMT1, ftsK-KOPSblind-Cm + pMS89	Transfer of ftsK-KOPSblind-Cm from VSO4(3)[†,§]
MS554	MS112 inter(trg;ydcI)::parS P1, inter(ydeU;ydeK)::parS pMT1, recA56::Tc + pMS11	Transfer of recA56[‖]
MS555	MS112 inter(ydeP;ydeQ)::parS P1, inter(ydgJ;ydgT)::parS pMT1, recA56::Tc + pMS11	Transfer of recA56[‖]
MS556	MS112 inter(ycgY;treA)::parS P1-Kn, inter(ydeU;ydeK)::parS pMT1, recA56::Tc + pMS11	Transfer of recA56[‖]
MS520	MS112 inter(trg;ydcI)::parS P1, inter(ydeU;ydeK)::parS pMT1, xerC::FRT-kn-FRT + pMS11	Transfer of xerC::FRT-kn-FRT from JW3784[†,¶]
MS543	MS112 inter(ydeP;ydeQ)::parS P1, inter(ydgJ;ydgT)::parS pMT1, xerC::FRT-kn-FRT + pMS11	Transfer of xerC::FRT-kn-FRT from JW3784[†,¶]
MS563	MS112 inter(trg;ydcI)::parS P1, inter(ydeU;ydeK)::parS pMT1, xerC::FRT-kn-FRT,recA56::Tc + pMS11	Transfer of recA56[‖]
MS564	MS112 inter(ydeP;ydeQ)::parS P1, inter(ydgJ;ydgT)::parS pMT1, xerC::FRT-kn-FRT,recA56::Tc + pMS11	Transfer of recA56[‖]
MS537	MS112 inter(trg;ydcI)::parS P1, inter(ydeU;ydeK)::parS pMT1, ftsK ATP-::cm + pMS89	Transfer of ftsK ATP- Cm(3)[†]
MS538	MS112 inter(ydeP;ydeQ)::parS P1, inter(ydgJ;ydgT)::parS pMT1, ftsK ATP-::cm + pMS89	Transfer of ftsK ATP- Cm(3)[†]
MS557	MS112 inter(trg;ydcI)::parS P1, inter(ydeU;ydeK)::parS pMT1, ftsK delC::Tc + pMS11	Transfer of del(ftsKC)::Tc (3)[†]
MS540	MS112 inter(ydeP;ydeQ)::parS P1, inter(ydgJ;ydgT)::parS pMT1, ftsK delC::Tc + pMS11	Transfer of del(ftsKC)::Tc (3)[†]

St, streptomycin resistance determinant; Kn, kanamycin resistance deteminant; Gm, gentamycin resistant determinant; Cm, chloramphenicol resistance determinant; Tc, tetracyclin resistance determinant.

*Transgenesis using plasmids of the pLN135 family used an integration-excision procedure described in ref. 1.

[†]Constructs tagged by resistance determinants were transferred by P1 transduction following standard procedures.

[‡]Red-mediated transgenesis was done in strain DY378 following standard procedures (5) and then were transferred to relevant strains by P1 transduction.

[§]Unless specified (parS P1-Kn), the parS P1-FRT-Cm-FRT and parS pMT1-FRT-Cm-FRT cassettes were first inserted or transferred into relevant strains, and then the Cm determinant was deleted using plasmid pCP20 (6).

[¶]The KEIO collection of E. coli gene deletion mutants is described in ref. 7.

[‖]The recA56-null allele was cotransferred by conjugation with an srl::Tn10 insertion from strains JC10240 ((Hfr PO45 recA56 srl::Tn10 thr300 ilv318 rpl300; our strain collection).

1. Cornet F, Louarn J, Patte J, Louarn J (1996) Restriction of the activity of the recombination site dif to a small zone of the Escherichia coli chromosome. *Genes Dev* 10(9):1152–1161.
2. Reyes-Lamothe R, Possoz C, Danilova O, Sherratt D (2008) Independent positioning and action of Escherichia coli replisomes in live cells. *Cell* 133(1):90–102.
3. Sivanathan V, et al. (2009) KOPS-guided DNA translocation by FtsK safeguards Escherichia coli chromosome segregation. *Molecular Microbiology* 71(4):1031–1042.
4. Barre F, et al. (2000) FtsK functions in the processing of a Holliday junction intermediate during bacterial chromosome segregation. *Genes Dev* 14(23):2976–2988.
5. Yu D, et al. (2000) An efficient recombination system for chromosome engineering in Escherichia coli. *Proc Natl Acad Sci USA* 97(11):5978–5983.
6. Datsenko KA, Wanner BL (2000) One-step inactivation of chromosomal genes in Escherichia coli K-12 using PCR products. *Proc Natl Acad Sci USA* 97(12):6640–6645.
7. Baba T, et al. (2006) Construction of Escherichia coli K-12 in-frame, single-gene knockout mutants: The Keio collection. *Mol Syst Biol* 2:2006.0008.

Table S2. Plasmids used

Plasmid	Relevant genotype, construct	Comments
pALA2705	lacZp–gfp–parB P1, ApR	(1)
pFHC2973	lacZp–ecfp–parB P1–yfp–parB pMT1, ApR	(1)
pLN135	pSC101 derived, repATs,rpsL+, CmR	Transgenesis vector (2)
pMS7	pLN135 with an engineered lacI–lacY region deleted for lacZ	For Plac-driven constructs at the lacZ locus
pMS8	pMS7 with gfp–parB P1	For Integration of gfp–parB P1 at the lacZ locus or use for plasmid-driven expression
pMS11	pMS7 with mCherry–parB pMT1	For Integration of mCherry parBpMT1 at the lacZ locus or use for plasmid-driven expression
pMS89	pMS11 with a Kn resistance determinant	For plasmid-driven expression in Cmresistant strains
pMS1	pUC57 (Genscript) with a modified multiple cloning site linker, ApR	Cloning vector
pMS24	pMS1 with a parS P1–Kn cassette	Source of parS P1–Kn cassette
pGKD3–parS P1	pGB2 derivative carrying a parS P1–FRT–Cm–FRT cassette	Source of parS P1–FRT–Cm–FRT cassette (3)
pGKD3–paS pMT1	pGB2 derivative carrying a parS pMT1–FRT–Cm–FRT cassette	Source of parS pMT1–FRT–Cm–FRT cassette (4)
pMS27	pMS1 with a 4.8-kb fragment from pFX240 containing 192 tetO sites and Gm	Source of tetO–Gm cassette. pFX240 is a gift from F.-.X. Barre (Centre National de la Recherche Scientifique, Gif-sur Yvette, France)
pMS34	pLN135 with an engineered ydeE–ydeH locus	For cloning cassettes at the ydeE–ydeH locus
pMS35	pLN135 with an engineered ydgJ–ydgT locus	For cloning cassettes at the ydgJ–ydgT locus
pMS38	pLN135 with an engineered ycgY–treA locus	For cloning cassettes at the ycgY–treA locus
pMS29	pLN135 with an engineered ydbL–feaR locus	For cloning cassettes at the ydbL–feaR locus
pMS42	pLN135 with an engineered gdhA– ynjL locus	For cloning cassettes at the gdhA–ynjL locus
pMS43	pLN135 with an engineered yffS–eutA locus	For cloning cassettes at the yffS–eutA locus
pMS44	pLN135 with an engineered ilvA–ilvY locus	For cloning cassettes at the ilvA–ilvY locus
pMS45	pLN135 with an engineered ybhC–ybhJ locus	For cloning cassettes at the ybhC–ybhJ locus
pMS46	pMS34 with the tetO–Gm cassette	For Integration of tetO–Gm at the ydeE–ydeH locus
pMS47	pMS29 with the tetO–Gm cassette	For Integration of tetO–Gm at the ydbL–feaR locus
pMS48	pMS35 with the tetO–Gm cassette	For Integration of tetO–Gm at the ydgJ–ydgT locus
pMS49	pMS38 with the tetO–Gm cassette	For Integration of tetO–Gm at the ycgY–treA locus
pMS50	pMS42 with the tetO–Gm cassette	For Integration of tetO–Gm at the gdhA–ynjL locus
pMS53	pMS45 with the tetO–Gm cassette	For Integration of tetO–Gm at the ybhJ–ybhC locus
pMS55	pMS38 with parS P1–Kn cassette	For Integration of parS P1–Kn at the ycgY–treA locus
pMS56	pMS43 with parS P1–Kn cassette	For Integration of parS P1–Kn at the yffS–eutA locus
pMS57	pMS35 with parS P1–Kn cassette	For Integration of parS P1–Kn at the ydgJ–ydgT locus
pMS58	pMS45 with parS P1–Kn cassette	For Integration of parS P1–Kn at the ybhC–ybhJ locus
pMS59	pMS44 with parS P1–Kn cassette	For Integration of parS P1–Kn at the ilvA–ilvY locus

1. Nielsen HJ, Ottesen JR, Youngren B, Austin SJ, Hansen FG (2006) The Escherichia coli chromosome is organized with the left and right chromosome arms in separate cell halves. *Mol Microbiol* 62(2):331–338.
2. Cornet F, Louarn J, Patte J, Louarn J (1996) Restriction of the activity of the recombination site dif to a small zone of the Escherichia coli chromosome. *Genes Dev* 10(9):1152–1161.
3. Espeli O, Mercier R, Boccard F (2008) DNA dynamics vary according to macrodomain topography in the E. coli chromosome. *Mol Microbiol* 68(6):1418–1427.
4. Mercier R, et al. (2008) The MatP/matS site-specific system organizes the terminus region of the E. coli chromosome into a macrodomain. *Cell* 135(3):475–485.

Table S3. Insertion used for loci positioning

Region	Tagged loci*	Insertion site†	Site inserted
ori	***ilvA****-ilvY*	3,954,537 bp, GGCCTACCCG▼CGCGACAACG	parS-P1
left	***yffS****-eutA*	2,563,422 bp, GCACCACAAT▼TACCCCAACC	parS-P1
right	***ybhJ****-ybhC*	805,098 bp, TAAGGCATTT▼TCGCAGCATC	parS-P1, parS-pMT1, tetO array
ter	***ycgY****-treA*	1,244,862 bp, ACAACGCCAT▼CCGGAGAAGC	parS-P1, parS-pMT1, tetO array
ter	***ydbL****-feaR*	1,444,309 bp, AATATTCAAA▼AACTCCTGTC	tetO array
ter	***ydcB****-trg*	1,490,280 bp, CGAAAATAAT▼CACTTCACGA	parS-P1, parS-pMT1
ter	***ydeP****-ydeQ*	1,584,724 bp, TCTTACAGGT▼GTAGGCTAAT	parS-P1, parS-pMT1
ter	***ydeU****-ydeK*	1,592,139 bp, TTGCCGACTT▼CAAACGGCGC	parS-P1, parS-pMT1
ter	***ydeE****-ydeH*	1,620,588 bp, TCGTTTAGGT▼TACCTCTGCT	tetO array
ter	***ydgJ****-ydgT*	1,702,639 bp, TGCTGGAGCT▼ATTATTGCTA	parS-P1, parS-pMT1, tetO array
ter	***arpB****-ydiY*	1,803,178 bp, GAGATATGCA▼GGACACTGGT	parS-pMT1
ter	***gdhA****-ynjL*	1,841,750 bp, GGCCTACAAA▼TGGGCACAAT	tetO array

*Sites were inserted in intergenic regions of converging genes and named after the first gene (bolded).
†The insertion coordinates are given (in bp) with the surrounding sequence (arrowheads show the insertion position).